FOLZ). This is in good agreement with Fig. 5(*a*) of Lehmpfuhl, Krahl & Uchida (1995). The anomalous behaviour in the HOLZ-line intensities for $D = 0.46$ Å^2 found by Lehmpfuhl, Krahl & Uchida (1995) is not present.

The value of $D = 0.46$ Å^2 (Aldred & Hart, 1973) used in the simulations is consistent with other experimental evidence (Butt & Bashir, 1988) and gave excellent agreement with the experimental zero-order CBED patterns for both [111] and [100] zone axes when the Einstein model was used to represent the absorption due to TDS (provided that this is not included perturbatively). Therefore, our calculations suggest that no anisotropy in the Debye–Waller factor should be concluded from the experimental results of Lehmpfuhl, Krahl & Uchida (1995). This is consistent with theoretical expectations that, for silicon at room temperature, anharmonic contributions to the Debye–Waller factor should be small (Sears & Shelley, 1991).

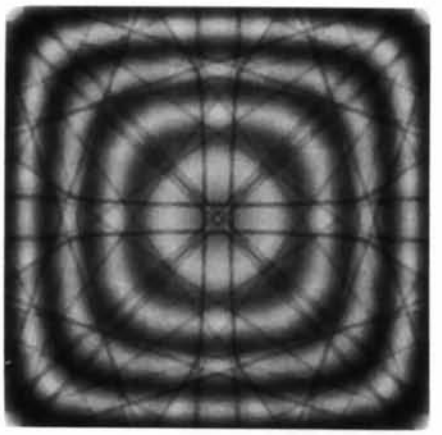

Fig. 2. Zero beam of CBED pattern near [100] zone axis showing FOLZ lines. The wavelength is 0.03718 Å and the thickness 2720 Å. 93 beams were used and absorption included using the Einstein model, $D = 0.46$ Å^2.

References

Aldred, P. J. & Hart, M. (1973). *Proc. R. Soc. London Ser. A*, **332**, 223–254.

Allen, L. J. & Rossouw, C. J. (1989). *Phys. Rev. B*, **39**, 8313–8321.

Allen, L. J. & Rossouw, C. J. (1990). *Phys. Rev. B*, **42**, 11644–11654.

Bird, D. M. & King, Q. A. (1990). *Acta Cryst.* A**46**, 202–208.

Butt, N. M. & Bashir, J. (1988). *Acta Cryst.* A**44**, 396–398.

Doyle, P. A. & Turner, P. S. (1968). *Acta Cryst.* A**24**, 390–397.

Hall, C. R. & Hirsch, P. B. (1965). *Proc. R. Soc. London Ser. A*, **286**, 158–177.

Ichimiya, A. & Lehmpfuhl, G. (1978). *Z. Naturforsch. Teil A*, **33**, 269–281.

Lehmpfuhl, G., Krahl, D. & Uchida, Y. (1995). *Acta Cryst.* A**51**, 504–514.

Rez, D., Rez, P. & Grant, I. (1994). *Acta Cryst.* A**50**, 481–497.

Sears, V. F. & Shelley, S. A. (1991). *Acta Cryst.* A**47**, 441–446.

Voss, R., Lehmpfuhl, G. & Smith, P. J. (1980). *Z. Naturforsch. Teil A*, **35**, 973–984.

Waasmeier, D. & Kirfel, A. (1995). *Acta Cryst.* A**51**, 416–431.

Acta Cryst. (1996). A**52**, 498–499

X-ray topography of a lysozyme crystal

V. STOJANOFF* AND D. P. SIDDONS *at NSLS, Brookhaven National Laboratory, Upton, New York 11973, USA. E-mail: vstojan@bnlarm.bnl.gov*

(*Received 1 August 1995; accepted 2 January 1996*)

Abstract

X-ray topography methods were employed to identify defects in lysozyme crystals. White-beam and monochromatic topographs of lysozyme crystals obtained at the National Synchrotron Light Source are presented.

X-ray topography is a well established technique to characterize growth- or process-induced defects. Introduced in the late 40's and early 50's by Guinier & Tennevin (1949) and by Schultz (1954), X-ray topography as we know it today derives from the techniques developed by Lang (1958), Bond & Andrus (1952) and Bonse & Kappler (1958). A review of the theoretical background and the experimental techniques for X-ray topography was presented by Tanner (1976). With the advent of synchrotron-radiation sources, X-ray topography became largely employed in material characterization. The work by Tuomi, Naukkarinen & Rabe (1974) and Hart (1975) reflects the initial stage of the application of X-ray topography to the study of as-grown or process-induced defects in materials. The purpose of the present report is to show that X-ray topography can be a valuable tool in the study and understanding of protein growth conditions and diffraction properties.

White and monochromatic synchrotron radiation from beam line X26C at the National Synchrotron Light Source (NSLS) at Brookhaven National Laboratory were employed in X-ray topographic studies of defects in protein crystals. The X26C port was 20 m from the bending magnet and the spot size at the sample was 1 mm^2. For white-beam X-ray topography, the sample-to-film distance was of the order of 50 cm with an average exposure time of 30 s. The distance was chosen in order to avoid spot overlaps, however, the geometric resolution was decreased. In monochromatic synchrotron X-ray topography studies, a channel-cut (111) silicon crystal was employed. The crystal-to-film distance was about 10 cm and the exposures took several minutes. The geometrical resolution with the

monochromator was of the order of 3 μm. In both cases, a helium-filled volume between the sample and an acceptance slit was used to reduce scattering by air. The film was kept normal to the incident-beam direction.

Several measurements were carried out on tetragonal hen egg white lysozyme crystals ($a = b = 79.1$, $c = 37.9$ Å) grown by the hanging-drop method, sodium chloride and sodium acetate condition, pH 4.7. The crystal size fluctuated between 0.7 and 0.5 mm in all three directions. The first experiment, on room-temperature-grown and -stored crystals, showed highly strained regions; it was impossible to distinguish any individual kind of defect. For subsequent experiments, crystals grown and stored at constant temperature [288 (2) K] were used. In Fig. 1, a white-beam X-ray topograph of a lysozyme crystal is shown. Regions with a high density of defects and quite perfect regions can be observed in the topograph. Fig. 2 shows a monochromatic X-ray topograph of another lysozyme crystal. In this topograph, single dislocation lines as well as regions with high dislocation density can be identified. These crystals were used for data collection at a monochromatic diffraction station. The average mosaicity found for these crystals with no corrections applied was of the order of 0.01°. When compared to the mosaicity obtained from crystals grown under the same conditions but not submitted to X-ray topographic studies, the values were essentially the same, within 5% of the experimental errors. Recently, Fourme, Ducruix, Ries-Kautt & Capelle (1995) probed the quality of protein crystals by recording the Bragg profile of reflections of hen egg white lysozyme. These authors recorded the Bragg spot on film at the maximum-intensity condition. The images obtained agree with the images observed in the early stages of the present report when no internal structure could be observed in the crystals.

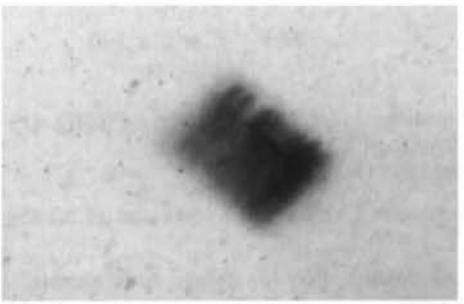

Fig. 1. White-beam X-ray topograph of a lysozyme crystal grown by the hanging-drop method at 288 K and pH 4.7. A few dislocations can be observed in this topograph.

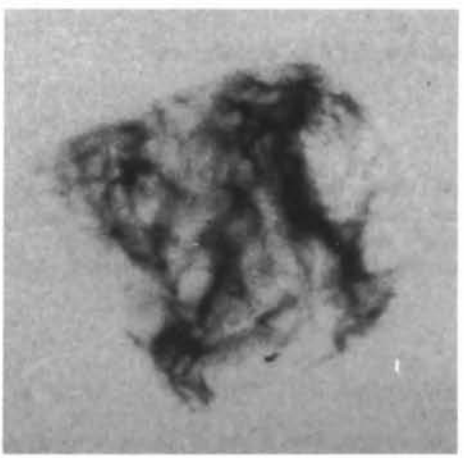

Fig. 2. Monochromatic synchrotron-radiation topograph ($\lambda = 1.1$ Å). Monochromator silicon channel cut, 111 reflection. Lysozyme crystal grown by the hanging-drop method at 288 K and pH 4.7. A net of single dislocations and a few highly strained regions can be identified.

It has been shown here that X-ray topography can be an important tool for evaluation of protein crystal quality and, at least for lysozyme crystals, it has been proved to be non-destructive. The relation between growth-induced defects and crystal structure determination will be reported elsewhere (Stojanoff, Siddons, Monaco, Vekilov & Rosenberger, 1996).

Discussions throughout this work with Dr F. Rosenberger, Dr L. Monaco and Dr P. Vekilov were greatly appreciated. The authors thank Ms G. Shea and the BioCars group for their technical support at the X26C beam line at the NSLS/BNL. They are also indebted to Mr D. Berman, Mr N. Tempel and Ms H. Kycia.

References

Bond, W. L. & Andrus, J. (1952). *Am. Mineral.* **37**, 622.
Bonse, U. & Kappler, E. (1958). *Z. Naturforsch. Teil A*, **13**, 348–349
Fourme, R., Ducruix, A., Ries-Kautt, M. & Capelle, B. (1995). *J. Synchrotron Rad.* **2**, 136–142.
Guinier, A. & Tennevin, J. (1949). *Acta Cryst.* **2**, 133–138.
Hart, M. (1975). *J. Appl. Cryst.* **8**, 436–444.
Lang, A. R. (1958). *J. Appl. Phys.* **29**, 597–598
Schultz, L. G. (1954). *J. Met.* **200**, 1082–1083.
Stojanoff, V., Siddons, D. P., Monaco, L., Vekilov, P. & Rosenberger, F. (1996). In preparation.
Tanner, B. K. (1976). *X-ray Diffraction Topography*, 1st ed. Oxford: Pergamon Press.
Tuomi, T., Naukkarinen, K. & Rabe, P. (1974). *Phys. Status Solidi A*, **25**, 93–106.